
Modelling trace metal (Hg and Pb) bioaccumulation in the Mediterranean mussel, *Mytilus galloprovincialis*, applied to environmental monitoring

Stellio Casas^{a,*} and Cédric Bacher^b

^aIFREMER, ZP de Brégallion, 83 140 La Seyne-sur-mer, France

^bIFREMER, BP 70, 29 280 Plouzané, France

*: Corresponding author : stellio_casas@yahoo.fr

Abstract

Bioaccumulation of metal within an organism results from interactions between physiological factors (growth, weight loss, absorption and accumulation), chemical factors (metal concentration, speciation and bioavailability) and environmental factors (temperature and food concentration). To account for such interactions in the mussel *Mytilus galloprovincialis*, we combined bioaccumulation and Dynamic Energy Budget models. Field experiments were conducted to measure uptake and elimination kinetics for two metals (Hg and Pb) in three Mediterranean sites with differences in contamination levels and to calibrate the models. Metal uptake from water and from food was considered separately. Metal elimination resulted from reproduction and/or from direct excretion. Contributions of physiological variables, such as body size and tissue composition were quantified. By combining environmental and biological data, the model provided an efficient bio-monitoring tool which can be applied to various coastal environments. An application to the French bio-integrator network (RINBIO) was carried out through inverse analysis and enabled to assess the real level of contamination in water on the basis of contamination measured in mussels.

Keywords: bio-indicator, Dynamic Energy Budget, inverse analysis, RINBIO

1 Introduction

Several monitoring programmes (such as US Mussel Watch, French RNO and RINBIO) are based on quantitative bio-indicator concept, using the ability of marine bivalves (usually mussels) to concentrate and, under certain conditions, accumulate contaminants in their tissues with respect to the ambient level. This technique is more efficient than direct measurements in the water (Goldberg, 1975; De Kock and Van het Groenewoud, 1985; Claisse et al., 1992; Andral et al., 2004). Nevertheless, interpreting bio-monitoring data reveals some difficulties related to the contaminant dynamics, possible changes in the environment (temperature, trophic conditions, contamination level) and interactions with the physiology of the animals.

First, metal levels in tissues represent a time-integrated response to bioavailable metal in food and water (Langston and Spence, 1995; Angelidis and Catsiki, 2002; Boisson et al., 2003). To estimate each flow, comparative studies of food and environmental contamination have been carried out in the laboratory, using tracer techniques to label algae and seawater (Fowler et al., 1971; 1978; Fowler, 1982; Borchardt, 1983; Clifton et al., 1983; Roesijadi et al., 1984; Borchardt, 1985; Lee et al., 1998; Roditi and Fisher, 1999; Boisson et al., 2003). The differences observed in the outcomes of these various studies outline the need for caution in predicting fluxes of metals such as Hg or Pb based solely on data derived from laboratory experiments. Experiments directly dedicated to metal kinetics of mussels in the natural environment, by measuring contamination in water and food, have not been carried out to date.

In addition, the resulting bioaccumulation is influenced by external environmental factors and internal biological processes (Rainbow et al., 1990; Wright, 1995; Lee and Luoma, 1998; Lee et al., 1998). Environmental factors include salinity, pH, redox potential, dissolved organic carbon, temperature and food availability (Bjerregaard and Depledge, 1994; Sunda and Huntsman, 1998). Significant internal biological factors include size, sex, sexual maturity, reproduction stages, and seasonal growth cycles (Wang and Eckmann, 1994). For example, as a proxy for the growth rate, the variation in tissue mass has been shown to produce large changes in metal concentrations in tissues, which the monitoring system must cope with. However, the relative influences of these biotic factors are not well documented, and the metal cycles within the animals not fully understood. This knowledge is a prerequisite for modelling bioaccumulation (Luoma

and Fisher, 1997) and for optimizing the use of bio-sentinel organisms in environmental monitoring programmes. In order to overcome the weight variation influence, some authors transformed metal concentrations into metal content for a virtual standard mussel (Boyden, 1977; Cossa et al., 1980; Riget et al., 1997) and others sampled mussels of uniform size (Popham and D'auria 1983; Andral and Stanisiere, 1999) or proposed to express the metal concentration per unit of shell mass (Fisher, 1983). None of these methods proved to be entirely satisfactory for monitoring purposes, owing to the limitations inherent to standardization methods, i.e. the combined effect of ageing, somatic growth and the reproduction cycle which cannot be easily distinguished.

However, the uptake/elimination model proposed by Kooijman and Van Haren (1990) for organic micro contaminants like PAH's (Polycyclic Aromatic Hydrocarbons) and PCB's (PolyChlorinated Biphenyls) has been designed to account for changes in the physiological (feeding/lipid) conditions of the organism. It is based on the Dynamic Energy Budget (DEB) model (Kooijman, 1986a; 1988; 1993; 2000) which describes growth, energy dynamics and reproduction as a function of body size. This modelling attempt suggests that bioaccumulation models could provide an appropriate tool to analyse bio-monitoring data.

The first purpose of this paper was to show how the DEB-based model could be applied to *M. galloprovincialis* to assess uptake-excretion kinetics for two high-priority metals, namely Hg and Pb. We took account of contaminant uptake from the environment, food concentration and excretion due to decontamination and spawning and we assessed the influence of physiological variables, such as body size and tissue composition on heavy metal kinetics. The model was calibrated and tested on field data, using mussels and environmental surveys in different sites and transferring mussels from clean to polluted sites. The second objective was to assess the real level of contamination of water on the basis of contamination measured in mussels in the French bio-integrator network (RINBIO). This innovative application of the model was carried out using an inverse method. Unknown food and contaminant concentrations were determined by fitting the simulated mussel growth and contaminant concentration to measured values. Extending this method to RINBIO sites produced a map of contaminant concentrations along the French Mediterranean coast.

2 Methods

2.1 Field data

2.1.1 Bio-monitoring data

RINBIO sites were located along 1,800 km of French Mediterranean shoreline (Fig. 1). The mussels were immersed for 3 months during their sexual dormancy period (between March and July). The choice also minimised the effect of bio-fouling to keep the moorings safe. The mussels came from an aquaculture farm in Languedoc-Roussillon (Aresquiers site). The 97 RINBIO bio-integrator network sites were immersed at the end of March, along 1800 km of French Mediterranean shoreline, and removed in July 2000 (Goldberg, 1975; De Kock and Van het Groenewoud, 1985; Claisse, et al., 1992; Andral et al., 2004). For each site, the mortality and several biometric parameters (length, width and height of the shell) were recorded for 30 individuals at the beginning and the end of the experiment. Several contaminants were measured in the mussels: lead, cadmium, copper, zinc, mercury, chrome, nickel, arsenic, dichlorodiphenyltrichlorethane (DDT, DDD and DDE), hexachlorocyclohexane (HCH), polychlorobiphenyles (PCB), and polycyclical aromatic hydrocarbons (PAH). The results were expressed in ng or µg of contaminants per gram of dry mussel tissue. Therefore, these national and international monitoring networks provided a large database that could be integrated in the DEB model to supply information about the nutritive quality of the water and the actual contamination of sites.

2.1.2 Field experiment

Field experiments on uptake and elimination kinetics were conducted in three Mediterranean sites selected on the basis of their contamination levels. Lazaret bay (43°05.40' N, 5°54.50' E) is subject one of the “hot spots” of heavy metal concentrations, particularly for Hg and Pb (Claisse 1989) (Fig. 1). Bages lagoon (43°04.70' N, 003°00.00' E) is particularly contaminated by cadmium (Claisse 1989) but not by Hg and Pb. Furthermore, Bages lagoon is a mesotrophic site where significant variability of trophic and physicochemical parameters is expected. This variability enabled us to explore the growth kinetics, in comparison with those of Lazaret, which is an oligotrophic site. Because of their respective contamination by Hg and Pb and their different trophic environments, Lazaret bay and Bages lagoon are appropriate sites for understanding

growth, bioaccumulation and related kinetics. In order to examine decontamination kinetics, a third site was selected, in a particularly clean environment in Port-Cros National Park ($43^{\circ}00.91' N$, $6^{\circ}23.41' E$). In this site, metal contamination is very low or even absent (Andral et al., 2004).

All mussels with 60 mm shell size were purchased from the same aquaculture farm (Aresquiers site) located in a clean, open site on the coast. Mussels were put into polyethylene net cages divided into three compartments containing 6 samples of 10 kg each. The cages were immersed at 10-12 m depth and suspended on fixed rearing structures (called "tables") or on buoys by ropes. The mussels were transferred from a clean to highly contaminated area, and then transferred back to the clean site. The experiments were designed to explore the kinetics of Hg in mussels with simultaneous measurements of metal concentrations in water and suspended particles, and measurements of mussel biometry. It allowed us to simultaneously observe metal accumulation and physiological changes in mussels. For the contamination experiments, mussels were transferred for six months to two contaminated sites (Lazaret bay and Bages lagoon), and fifty individuals from both sets were sampled fortnightly from mid September 2002 to mid March 2003. An additional transfer experiment was performed between mid December 2002 and mid March 2003, in order to explore the reproducibility of the experiment during a shorter period (Casas, 2005). At the end of these experiments, the cages were transported in cool containers to the clean site (Port-Cros Island) in order to examine the decontamination kinetics over three months (March 2003 to June 2003). Therefore, the experimental design included 4 populations equivalent to 4 datasets: population 1 was placed in Bages for 6 months then in Port-Cros for 3 months, population 2 was put in Bages for 3 months then in Port-Cros for 3 months, population 3 was put in Lazaret for 6 months then in Port-Cros for 3 months and population 4 was placed in Lazaret for 3 months then in Port-Cros for 3 months (Fig. 2).

For each fortnightly measurement, 30 mussels were collected on each site, were separated and rinsed in seawater. Several biometric parameters were recorded: length, width and height of the shell. At each site, samples were pre-processed according to standardised procedures (Claisse et al., 1992). The mussels were opened alive and the tissue was removed with a stainless steel scalpel. Shells were dried at $60^{\circ}C$ for 48 h. Mussel tissues were pooled, weighed and frozen in a cleaned 50 ml jar, then dried. Dried tissues were analyzed using different techniques of atomic absorption

spectrometry: Pb, Cd by flame atomic adsorption spectrometry; Hg by atomic fluorescence. The detailed procedure is described elsewhere (Chiffolleau et al., 2002; Cossa et al., 2002). Results were expressed in ng or µg of contaminants per gram of dry mussel tissue.

Temperature, salinity, pH and dissolved oxygen of the surface water were measured weekly in Lazaret bay, Bages lagoon and Port-Cros Island. Water samples were also collected and taken to the laboratory to analyse suspended particulate matter (SPM), chlorophyll-a, pheopigments, POC, ammonia (NH_3), nitrate (NO_3), nitrite (NO_2) and phosphate (Casas, 2005). During mussel sampling, water samples were also collected and transported to the laboratory to measure the dissolved and particulate concentrations of Hg and Pb.

2.2 *Model simulations*

2.2.1 *DEB growth model*

DEB models are based on simple assumptions about the rates at which the organism acquires energy from its environment, and on the rules describing how available energy is distributed between maintenance, growth and reproduction (Fig. 3). A summary of the DEB-model is given below and the parameters are listed in Tables 1 and 2. The notation and symbols follow those in Kooijman (2000) whereby the following main rules apply:

- variables are indicated by symbols and lower case symbols frequently relate to upper case ones via scaling;
- quantities are expressed per unit of volume with square brackets []; per unit of biosurface area with braces {};
- rates have dots, indicating the dimension per time.

Environmental concentrations (e.g. food, contaminant) are noted with a single letter. The dynamics of growth and reproduction were represented by differential equations of three state variables: structural body volume V (cm^3), energy reserves E (J) and energy allocated to development and reproduction R (J).

For a single food source, assimilation energy rate is a function of food concentration (X , mg.l^{-1}) and is proportional to surface area of the structural body

volume, which corresponds to the part of tissue without gonads and reserves. It is equal to:

$$\dot{p}_A = \{\dot{p}_{Am}\} \cdot f \cdot V^{2/3} \quad (\text{J.d}^{-1}) \quad [1]$$

$$\text{with } f = \frac{X}{X + X_K} \text{ and } \{\dot{p}_{Am}\} = (1 - \rho) \cdot \{\dot{p}_{Xm}\} \quad (\text{J. cm}^{-2} \text{d}^{-1})$$

where f is the functional response of assimilation to food concentration (dimensionless), X_K is the half saturation coefficient ($\mu\text{g pheopigment .l}^{-1}$) and $\{\dot{p}_{Am}\}$ is the maximum surface area-specific assimilation rate ($\text{J. cm}^{-2} \text{d}^{-1}$), ρ is the loss due to digestion, $\{\dot{p}_{Xm}\}$ is the maximum ingestion rate ($\text{J.cm}^{-2}.\text{d}^{-1}$).

Assimilation contributes to the dynamics of the energy reserves which are given by the equation:

$$\frac{dE}{dt} = \dot{p}_A - \dot{p}_C \quad (\text{J.d}^{-1}) \quad [2]$$

where \dot{p}_C (J.d^{-1}) denotes the energy utilisation rate.

Stored energy is mobilised from the reserves and is allocated to growth, maintenance and reproduction. A fixed fraction (κ) of energy used is allocated to somatic maintenance and growth while the remainder ($1 - \kappa$) is used for maturation/reproduction and maturity maintenance. Maintenance has priority over growth, so growth ceases when the food concentration is low. From this energy allocation rule, it follows that growth investment is given by:

$$\frac{dV}{dt} = \frac{\kappa \cdot \dot{p}_C - [\dot{p}_M]V}{[E_G]} \quad (\text{cm}^3.\text{d}^{-1}) \quad [3]$$

where $[\dot{p}_M]$ is the maintenance cost ($\text{J.cm}^{-3}.\text{d}^{-1}$), $[E_G]$ is the volume-specific cost for structure (J.cm^{-3}), and κ (-) is the fraction of energy utilisation rate spent on maintenance plus growth. Kooijman (2000) derived the following equation of energy utilisation from theoretical considerations:

$$\dot{p}_C = \frac{[E]}{[E_G] + \kappa \cdot [E]} \left(\frac{[E_G] \cdot \{\dot{p}_{Am}\} \cdot V^{2/3}}{[E_m]} + [\dot{p}_M] \cdot V \right) \quad (\text{J.d}^{-1}) \quad [4]$$

where $[E]$ represents energy density ($[E] = \frac{E}{V}$, J.cm⁻³) and $[E_m]$ is the maximum energy density in the reserve compartment.

Juvenile development (*i.e.* increase in state of maturity) and adult reproduction (*i.e.* gamete production and spawning) correspond to 2 different stages in the individual life history. The transition between juveniles and adults implies a change in the maintenance rate. Kooijman (2000) introduced a threshold value of the structural volume V_p which marks the transition between development and gamete production and showed that:

$$\frac{dR}{dt} = (1 - \kappa) \cdot \dot{p}_c - \left(\frac{1 - \kappa}{\kappa} \right) \cdot \min(V, V_p) \cdot [\dot{p}_M] \quad [5]$$

Spawning was triggered at a given date corresponding to observations of dramatic decrease of mussel dry mass. Following Pouvreau et al. (2006) we added an equation that would allow the reproduction compartment to decrease when the maintenance cost of the structural volume exceeds energy available for growth.

Shell length L (cm) was obtained from body volume using an allometric function:

$$L = \frac{V^{1/3}}{\delta_m} \quad (\text{cm}) \quad [6]$$

where δ_m is the shape coefficient.

Fresh tissue mass W (g) was obtained by summing the 3 variables E (J), V (cm³) and R (J) after conversion into fresh mass. A specific mass d of 1 g.cm⁻³ was used to convert volume into mass:

$$W = d \cdot \left(V + \frac{E}{[E_G]} + \frac{R}{[\mu_E]} \right) \quad (\text{g}) \quad [7]$$

$\{\dot{p}_{Am}\}$ and $[\dot{p}_M]$ are given for a temperature of 20°C, and temperature dependence is defined by an exponential function based on the Arrhenius temperature of $T_A = 5800$ K, which would be approximately the same as a Q₁₀ factor of 2.67, as shown below:

$$\dot{k}(T) = \dot{k}_1 \exp \left\{ \frac{T_A}{T_1} - \frac{T_A}{T} \right\} \cdot \left(1 + \exp \left\{ \frac{T_{AL}}{T} - \frac{T_{AL}}{T_L} \right\} + \exp \left\{ \frac{T_{AH}}{T_H} - \frac{T_{AH}}{T} \right\} \right)^{-1} \quad (\text{-}) \quad [8]$$

where \dot{k} is a physiological rate (e.g. $\{\dot{p}_{Am}\}, [\dot{p}_M]$) at temperature T , \dot{k}_1 the same rate at the reference temperature T_1 which has been set here to 293 K and T_A is a species-specific coefficient, the so-called Arrhenius temperature (K). T_L is the lower boundary of tolerance range, T_H the upper boundary of tolerance range, T_{AL} and T_{AH} the Arrhenius temperatures (K) for the rate of decrease at both boundaries.

Parameter values were assessed from independent datasets on *M. edulis* by Van der Veer et al. (2006) and are summarised in Tables 1 and 2. We assumed that the same parameter values are valid for *M. galloprovincialis*, which is reasonable for 2 reasons: *i*) both species are cultivated in France and have similar growth rates and living areas, *ii*) our modelling exercise showed a good agreement between observed and simulated growth for *M. galloprovincialis*.

2.2.2 DEB bioaccumulation model

In addition to DEB equations, a model of heavy metal kinetics has been established. Contrary to models used for organic compounds (Kooijman and van Haren 1990; van Haren, Schepers et al. 1994), which may be lipophilic, the specific partition is not integrated between the aqueous fraction, the stored energy body compartment and the structural volume compartment (Fig. 3). The chemical affinity of the xenobiotic is incorporated. Uptake and elimination rates are both assumed to be proportional to the surface area of the isomorphic animal $V^{2/3}$ (Devillers et al., 1998) for a discussion on the proportionality of ingestion with respect to the surface area). Uptake from water is proportional to the surface area, because isomorphism links the surface area of gills, for instance, to the total surface area.

Following the notations from Van Haren et al. (1994), the resulting differential equation for the metal concentration (C_w) based on fresh tissue mass ($\text{mg} \cdot \text{kg}^{-1}$) is given by:

$$\frac{dC_w}{dt} = \frac{(\dot{r}_{da} \cdot C_d + \dot{r}_{pa} \cdot f \cdot C_p) \cdot V^{2/3}}{W} - \frac{\dot{r}_{ad} \cdot C_w \cdot V^{2/3}}{W} - \frac{C_w}{W} \cdot \frac{dW}{dt} \quad (\text{mg} \cdot \text{kg}^{-1} \cdot \text{day}^{-1}) [9]$$

where \dot{r}_{da} and \dot{r}_{pa} are the uptake rates for water ($\text{L} \cdot \text{cm}^{-2} \cdot \text{day}^{-1}$) and food ($\text{g} \cdot \text{cm}^{-2} \cdot \text{day}^{-1}$), \dot{r}_{ad} is the elimination rate constant ($\text{g} \cdot \text{cm}^{-2} \cdot \text{day}^{-1}$), $V^{2/3}$ is the surface derived from the body volume and W is the fresh tissue mass (g), C_d and C_p are the dissolved ($\mu\text{g} \cdot \text{L}^{-1}$) and

particulate ($\text{mg} \cdot \text{kg}^{-1}$) adsorbed metal concentrations which were interpolated from measurements (see below).

2.2.3 DEB parameter estimation

Most of the DEB parameters were derived from other studies (Van der Veer et al., 2006). Spawning time was imposed on the basis of observations and the initial conditions of the three compartments (structural volume, reserves and reproduction compartment) were unknown. The reserves compartment was estimated, the other two were calculated from the fresh tissue mass and shell length. The shape and half saturation coefficients were calibrated using food concentration and growth data from the 4 experimental datasets. The calibration was carried out with an algorithm based on the simplex method (Nelder and Mead, 1965) which consists in seeking the minimum of a function defining the average difference between simulated (Y_s) and measured (Y_o) dry tissue or fresh tissue mass:

$$\sum \left(\frac{Y_s - Y_o}{Y_o} \right)^2$$

The 4 bioaccumulation datasets of Hg and Pb were used to calibrate the three metal-specific kinetic rates: \dot{r}_{da} , \dot{r}_{pa} and \dot{r}_{ad} using the same method as that used for shape and saturation coefficients.

2.3 Inverse analysis

The coupled DEB-bioaccumulation model was used to assess the level of water contamination on the basis of the contamination measured in mussels with an inverse method. Unknown food and contaminant concentrations were determined by fitting simulated mussel growth and contaminant concentrations to measured values. By extending this method to RINBIO sites, we obtained a map of contaminant concentrations along the French Mediterranean coast. Growth measurements of initial tissue mass and shell height at time t_0 , final tissue mass and shell height at time $t_{+3\text{months}}$, and water temperature were combined with the DEB model to estimate the functional response (f) at each RINBIO site. In a second step, the initial and final metal

concentrations measured in mussels were used to estimate the concentration of contaminants in the water assuming no variation over time. In fact, there are two unknown factors, which are the water metal concentration in dissolved and particulate forms. Inverse analysis was first performed to obtain the uptake parameter U from the model equation.

$$U = \dot{r}_{da} \cdot C_d + \dot{r}_{pa} \cdot f \cdot C_p$$

The dissolved (C_d) and particulate (C_p) parts could not be determined but, since RINBIO measurements are carried out in summer under oligotrophic conditions, we assumed that Hg and Pb dissolved fractions were the major source of contamination. The results of Hg and Pb concentrations estimated by inverse analysis for Lazaret, Bages and Port-Cros were compared to the values measured during our contamination experiments.

3 Results

3.1 Field data

3.1.1 Hydrological and chemical data

During the contamination experiment the water temperature in both Lazaret and Bages showed a decrease from respectively 22.9°C at the beginning of the experiment to a minimum of 11.4°C in Lazaret bay and from 22.9°C to 3.6°C in Bages (Fig. 4a).

Chlorophyll-a and pheopigments showed variability in both areas with the highest average concentration in Bages, of respectively 1.45 and 6.8 $\mu\text{g.l}^{-1}$ versus respectively 0.5 and 0.82 $\mu\text{g.l}^{-1}$ in Lazaret (Fig. 4b,c). In Lazaret, the significant peak on 11 October 2003 was related to a stormy event. The highest values of particulate matter were linked to the resuspension of particles due to excessive wind, wave action and rain and no seasonal cycle was detected. The changes in chlorophyll-a and pheopigment concentrations ranged from maximum values of 3 and 3.79 $\mu\text{g.l}^{-1}$ to a minimum of 0.025 $\mu\text{g.l}^{-1}$ (Fig. 4b). In Bages, a major peak was observed for pheopigments (13 February 2003) after a wind/rain event. Due to this situation, chlorophyll-a and pheopigment concentrations varied from maximum values of 20 and 57 $\mu\text{g.l}^{-1}$ respectively, to almost 0 (Fig. 4c).

Metal analyses in Lazaret water showed high levels of Hg and Pb ($1.98 \text{ } 10^{-3} \mu\text{g.l}^{-1}$ and $0.1 \mu\text{g.l}^{-1}$ respectively). The dissolved Hg concentration in Lazaret increased during the first period of the experiment then decreased slowly (not shown). Particulate Hg followed the same changes. In parallel, the Pb dissolved concentration increased from $16.9 \text{ } 10^{-3} \mu\text{g.l}^{-1}$ to $20 \text{ } 10^{-3} \mu\text{g.l}^{-1}$ while particulate Pb remained at the same level after a peak at the beginning (25 November 2003). Metal analyses in the water of Bages showed low levels of dissolved Hg and Pb ($0.48 \text{ } 10^{-3}$ and $19.85 \text{ } 10^{-3} \mu\text{g.l}^{-1}$, not shown). Overall, the mean concentration of Hg in Lazaret was 4 to 6 times higher than in Bages, and the Pb concentration was 5 to 7 times higher in Lazaret.

During the decontamination and in Port-Cros, temperatures varied from 13.5° (mid March) to 23.5°C at the end of the experiment (Fig. 4a). Chlorophyll-a and pheopigments remained almost constant, varying from 1.8 to ca. 0 for chlorophyll-a, and from 1.96 to ca. 0 for pheopigments (Fig. 4d). Heavy metal levels (dissolved and particulate) in water were low (not shown).

3.1.2 *Mussel growth*

In Lazaret, tissue mass slowly increased during the contamination experiment until December. At that time, a sharp drop in tissue mass of about 43 % was observed (Fig. 5), probably due to spawning. Tissue mass continued to slowly decrease during the following winter. The beginning of the decontamination experiment corresponded to the spawning period, showing a 26 % decrease in tissue. This was followed by a slow growth phase from March.

In Bages, tissue mass quickly increased during the contamination experiment until 21 November 2002. After that date, a sharp decrease was observed, with a mass loss of about 36 %, due to reproduction (Fig. 5). Then a rapid growth phase was noted. During decontamination experiment, the end of the spawning period was also observed at the same time with a small loss (3%) followed by a growth phase. This limited mass loss confirmed that the mussels were at the end of the spawning period when transferred. After their transfer to Port-Cros, a short growth phase and rapid drop in mass were observed (Fig. 5).

3.1.3 *Hg accumulation*

In Lazaret, the Hg accumulation curve resembled an asymptotic curve reaching pseudo-equilibrium (Fig. 6). Over the 6 months of exposure, uptake was steady except

between 9 and 16 December 2002, when a sharp rise in Hg concentrations in tissue, from 0.3 mg.kg^{-1} to 0.45 mg.kg^{-1} , was observed. Pseudo-equilibrium was reached after 110 days (0.5 mg.kg^{-1}). During the 3-month experiment, the pseudo-equilibrium (0.42 mg.kg^{-1}) was reached quite rapidly after 60 days. These two Hg accumulation curves were similar and reached a saturation plateau at the same time.

In Bages, the Hg concentrations in tissue did not show a significant accumulation (Fig. 6). The Hg concentration in tissue at the end of experiment (0.08 mg.kg^{-1}) was about 5 times lower than that of the contaminated site in Lazaret (0.45 mg.kg^{-1}). A change in concentration was observed in each location around December, 12th in relation with a substantial loss of tissue mass due to the spawning period. The Hg decontamination kinetics in the tissue of mussels transferred from Lazaret to Port-Cros was significant, with 23 % decrease after 103 days. Consistent with the absence of Hg contamination in Bages and Port-Cros, no Hg change in mussel tissue was observed after mussels were transferred from Bages to Port-Cros.

3.1.4 Pb accumulation

In Lazaret the Pb accumulation kinetics curve during the first experimental period (6 months) reached an asymptote around December 12th, after a significant increase from 4.3 mg.kg^{-1} to 6.9 mg.kg^{-1} occurred (Fig. 6). During the second experimental period (3 months), the Pb concentration leveled out around the 30th day, with a concentration of 6.5 mg.kg^{-1} . After this equilibrium, the following period was similar to the first, with a large drop in the concentration (6 mg.kg^{-1}).

In Bages, the Pb concentration remained constant, with a peak at mid-term (December 2002, 1.5 mg.kg^{-1}), reaching a final value of 0.8 mg.kg^{-1} which was slightly higher than the initial value of 0.5 mg.kg^{-1} . The Pb concentration was about 5 to 7 times lower than those at the contaminated site of Lazaret Bay (Fig. 6).

After mussels were transferred from Lazaret Bay to Port-Cros, the Pb decontamination was significant with a decrease of 40 % after 103 days (Fig. 6). Consistent with the absence of Pb contamination in Bages lagoon, no Pb changes in mussel tissue were observed after the transfer of mussels from Bages to Port-Cros and concentrations stayed lower than 1 mg.kg^{-1} .

3.2 Model simulations

3.2.1 DEB growth model

After calibration of X_k and δ_m using the 4 growth datasets, the simulations fitted to observed total mass with an average relative error lower than 9 % (Fig. 5). The estimated shape coefficient, δ_m , was 0.25 and the estimated value of X_k 3.88 $\mu\text{g.l}^{-1}$. Functional response f varied from 0 to 0.35 in Lazaret and Port-Cros site and from 0 to 0.9 in Bages site, depending on pheopigment trends over time (not shown). This showed that food concentrations could be limiting, especially in Lazaret and Port-Cros.

3.2.2 DEB bioaccumulation model

Calibration of the three kinetic rates (\dot{r}_{da} , \dot{r}_{da} and \dot{r}_{ad}) led to a model which was well fitted to the observed kinetics of Hg ($\dot{r}_{da} = 4.92 \text{ l cm}^{-2} \text{ d}^{-1}$, $\dot{r}_{pa} = 9 \cdot 10^{-4} \text{ g cm}^{-2} \text{ d}^{-1}$ and $\dot{r}_{ad} = 0.0156 \text{ g cm}^{-2} \text{ d}^{-1}$) and Pb ($\dot{r}_{da} = 1.73 \text{ l cm}^{-2} \text{ d}^{-1}$, $\dot{r}_{pa} = 1.6 \cdot 10^{-3} \text{ g cm}^{-2} \text{ d}^{-1}$ and $\dot{r}_{ad} = 0.0256 \text{ g cm}^{-2} \text{ d}^{-1}$). The goodness of fit of predicted Hg and Pb concentrations in mussels was satisfactory ($R^2 = 0.93$ for Hg and $R^2 = 0.73$ for Pb). The model correctly translated the differences in contamination between Lazaret, Bages and Port-Cros, and the different periods of these kinetics: accumulation, spawning, concentration, dilution, pseudo-equilibrium and decontamination. Some weakness in the Pb bioaccumulation model was observed primarily on the 3 months of accumulation in Bages. Indeed, over this period, the model underestimated the rapid accumulation, whereas the 3 other kinetics were well reproduced.

Flow assessment confirmed the distribution of each part of the bioaccumulation equation: flow of dissolved uptake, particulate uptake, elimination and the concentration/dilution process due to starvation/growth periods of the mussel. The model indicated higher input of Hg and Pb in their dissolved form rather than in particulate form. This was due to the fact that the contamination site studied was a stable oligotrophic site with low particle content. Concurrently, trophic conditions in Bages were better and low levels of Hg and Pb limited the particulate flow.

3.2.3 Inverse analysis

For each site the f parameter was estimated from the variations in growth - values varied between 0 (lower nutritive condition) and 1 (maximum nutritive condition). An east-west gradient was revealed, with an increase in the functional response value (and thus,

trophic quality) towards the West (Fig. 7). This gradient, contrary to that of temperature, proportionally influences and directly forces mussel growth. Maximum values of functional response over the RINBIO network were equal to 0.8 at Palavas (site number 15) and the minimum was ca. 0 (at eastward sites and lagoon sites) with an average of 0.25. A group of western open-sea sites (sites 2-22) had f values higher than 0.4; and a second group, including the eastern open-sea sites (sites 23-49) and lagoon sites (sites 78-90), had f value under 0.2.

Inverse analysis applied to Hg and Pb concentration in mussels yielded dissolved Hg concentrations in water which varied from a maximum of $2.1 \cdot 10^{-3} \mu\text{g.L}^{-1}$ (Lazaret, site 31) to a minimum of $0.18 \cdot 10^{-3} \mu\text{g.L}^{-1}$ (Fréjus, site 40), with a mean value of $0.43 \cdot 10^{-3} \mu\text{g.L}^{-1}$ (Fig. 7). Only 8 sites had a calculated concentration above $10^{-3} \mu\text{g.L}^{-1}$. The computed dissolved Pb concentrations in water showed a maximum of $107 \cdot 10^{-3} \mu\text{g.L}^{-1}$ (Lazaret, site 31) and a minimum of $4.3 \cdot 10^{-3} \mu\text{g.L}^{-1}$ (South Thau lagoon, site 83), with a mean value of $20 \cdot 10^{-3} \mu\text{g.L}^{-1}$. Only 4 sites had a calculated concentration higher than $40 \cdot 10^{-3} \mu\text{g.L}^{-1}$.

Since the three experimental sites (Lazaret bay, Bages lagoon and Port-Cros Island) belonged to the RINBIO network, we compared, predicted and measured values of Hg and Pb concentrations in the water and found that the inverse analysis was accurate (Table 3).

4 Discussion

4.1 DEB growth model

An existing DEB model to several existing datasets of environmental parameters (pheophytin, temperature) and mussel growth in 3 Mediterranean sites was applied and only two parameters were calibrated: the shape coefficient (δ_m), which was used to convert fresh tissue mass to length, and the half saturation coefficient (X_k) corresponding to the food concentration for which the assimilation rate is half its maximum value. Van der Veer et al. (2006) reported a value of 0.287 for the shape coefficient for mussels not very different from our value (0.25), showing that our results were consistent – it must also be noted that the differences we found are much lower than differences between species (e.g. 0.165 for *Crassostrea* (Bacher and Gangnery, 2006-this issue) or 0.365 for *Macoma* (Van der Veer et al., 2006). As for the half saturation coefficient X_k we found that a single value for the 4 datasets ($X_k = 3.88 \mu\text{g.l}^{-1}$)

would suffice to reproduce growth data. In a previous work (Casas, 2005), shape coefficients were also estimated for the different sites and different food sources (SPM, chlorophyll-a, pheopigment, particulate organic carbon) were tested but the use of pheopigments as a single food source yielded the best simulations. However, a correlation was found between X_k and pheopigment averaged on each site and period (Casas, 2005) which showed that the influence of food concentration was not entirely reproduced by our formulation and might be improved by combining other food sources (Dowd, 1997; Rouillon and Navarro, 2003). However, the combination of several food sources is a complex task and is difficult to determine in ecophysiological models (Barillé et al., 1997; Grant and Bacher, 1998; Chavez-Villalba et al., 2002). Most often authors consider a single food source (Ren and Ross, 2001) which can be justified under oligotrophic conditions.

The four experimental datasets were characterised by low or null growth related to low trophic conditions. Gangnery et al. (2004) reported much higher mussel growth in another Mediterranean lagoon where mussel farming is supported by POM concentrations around 1 mg.l^{-1} and chlorophyll-a concentrations around $1 \mu\text{g.l}^{-1}$ (Gangnery et al., 2004). Average chlorophyll-a was equal to 0.25 in Port Cros, 0.5 in Lazaret and 1.45 in Bages. The same difference between sites were found for pheopigments, and measurements of POC also confirmed that Bages had better trophic conditions than the 2 other sites (Casas, 2005) in which carbon or phytoplankton concentrations were too low to support mussel growth. When the DEB model was applied to the growth experiments, we found that food was limiting growth – e.g. the functional response was most often lower than 0.5. When compared to RINBIO datasets, for which only mussel growth was measured, large differences in growth were noted and the functional response varied from 0 to 1, with higher values on the western side of the French Mediterranean coast.

Our attempts to use the DEB model revealed that application of the DEB model would benefit from further validation. The same parameters as for *M. edulis* were kept but it may be anticipated that the fraction of utilised energy spent on maintenance/growth or the temperature ranges would differ since they are species-specific (Van der Veer et al., 2006). On the other hand, we expect that growth of *M. galloprovincialis* is not very different from *M. edulis* in temperate waters, and the fact that our model reproduced well mussel tissue mass is encouraging. For shell length our model was not very accurate. However, length was an additional variable which is not part of the DEB energy flowchart

– i.e. length is derived from DEB state variables, but does not play any role in energy flows or bioaccumulation. The only reason why length is kept as a variable of interest is that it is often measured and used as an indicator of mussel growth or physiological condition. Another issue is raised by the inter-individual growth variability we found in our dataset, combined to low growth and low trophic conditions which are probably also a reason why length changes were not always consistent with fresh tissue mass. Last, simulations are sensitive to initial values of the reserve, body volume and reproduction compartments and special attention has to be devoted to their estimation. In this context, energy allocation between reproduction and growth would have to be further investigated and we would recommend to measure accurately the reproduction effort in order to validate the DEB model. Undoubtedly, the model might be improved in the future by a thorough review of *M. galloprovincialis* ecophysiological parameters (with respect to DEB concepts).

4.2 DEB bioaccumulation model

Growth and reproduction are the main biological factors influencing the bioconcentration process. On one hand, spawning of mussels, corresponding to a significant loss of mass (up to 40 % of the tissue mass here), combined with the accumulation process, causes an abrupt increase in the Hg concentration in tissues. On the other hand, growth counteracts Hg accumulation and its increase significantly dilutes the Hg content in the organism. Our results showed that Hg and Pb uptake do not proceed linearly over time in mussels, unlike many studies in other bivalves (George and Coombs, 1977; Bjerregaard and Depledge, 1994; Wang and Eckmann, 1994). In our

model, the dissolved Hg uptake rate $\left(\dot{k}_u = \frac{\dot{r}_{da} \cdot V^{2/3}}{W} \right)$ ranged from 1.9 to 3.3 L.g⁻¹.d⁻¹ ($\dot{r}_{da} = 4.915 \text{ L.cm}^{-2}.\text{day}^{-1}$) and was close to laboratory measurements on *Mytilus edulis* – e.g. 5 l.g⁻¹.d⁻¹ (Thomann et al., 1995), 1.84-4.75 l.g⁻¹.d⁻¹ (Roditi and Fisher, 1999), and 2.3 l.g⁻¹.d⁻¹ (Roditi et al., 2000). Similarly, the elimination rate of Hg $\left(\dot{k}_e = \frac{\dot{r}_{ad} \cdot V^{2/3}}{W} \right)$ varied between 0.006 and 0.01 d⁻¹. This value is lower than the values obtained in laboratory studies – e.g. 0.05 d⁻¹ (Roditi and Fisher 1999; Roditi, Fisher et al. 2000). Finally, the growth rate effect on bioaccumulation was equal to 0.002 d⁻¹ (Thomann et al., 1995; Roditi and Fisher, 1999; Roditi et al., 2000; Roditi et al., 2000). In our model, this rate

was deduced from the relation $\left(\frac{1}{W} \frac{dW}{dt} \right)$ and varied between a negative value of -0.015 d⁻¹ (dilution effect) and a positive value of 0.046 d⁻¹ (concentration effect). For Pb, the dissolved uptake rate \dot{k}_u varied between 0.6 and 1.14 l.g⁻¹.d⁻¹ which was comparable to results from (Thomann et al., 1995) ($\dot{k}_u = 1$ l.g⁻¹.d⁻¹). In our study, the elimination rate fell between 0.009 and 0.017 d⁻¹, thus in accordance with values obtained in lab studies: 0.001 d⁻¹ (Schulz-Baldes, 1977), 0.013 d⁻¹ (Thomann et al., 1995), 0.019-0.028 d⁻¹ (Fisher et al., 1996).

The uptake and elimination rate values calculated here were similar to lower values found in laboratory studies. The effect of growth on bioaccumulation was the only underestimated parameter. Uptake rates may be overestimated and growth effect underestimated in lab studies, due to the short duration of experiments (15-30 days), without reaching pseudo-equilibrium. Thus, only the first rapid period of uptake was observed and the physiological condition was not taken into account.

4.3 Inverse analysis: monitoring tool

Application of the model by inverse analysis to monitoring data (RINBIO) showed the usefulness of the DEB model as an operational tool. The model linked concentrations in the living organism with that of the surrounding environment using an explanatory method. It provided an evaluation of the effective chemical contamination on sites which have different trophic conditions in the Gulf of Lions by accounting for differences in physiological response. An integrated vision on the bioaccumulation process, with its spatial and temporal variations, was thus used and yielded information on the coastal contamination level. The successful reconstruction of Hg and Pb concentrations in surrounding water at different sites with concentrations in tissues and the measurement of growth encourage the implementation of the DEB-based model in scenario simulation studies for management purposes.

Our inverse analysis stresses the various Hg and Pb contaminations of the Mediterranean coast. Lazaret bay particular stands out with high contamination by dissolved Hg (Hg = 2.1 10⁻³ µg l⁻¹) and Pb (Pb = 107 10⁻³ µg l⁻¹). This site is impacted by intense maritime traffic and is defined as one of the “hot spots” of heavy metal concentrations, particularly for Hg and Pb (Claisse, 1989). Use of Pb in antifouling paints and petrol is still authorised by French legislation for ships over 25 m in length. This site

should receive detailed attention seeing its high levels of contamination. Near this bay, the concentrations in water predicted by the model sharply decreased (see site number 30, Hg = $1.3 \cdot 10^{-3} \mu\text{g l}^{-1}$, Pb = $26.7 \cdot 10^{-3} \mu\text{g l}^{-1}$) but remained high, showing the dilution of the contaminants in the sea. The high contamination of this site is thus related to the large input of contaminants from the harbour and industrial activities of the area and to limited water exchanges with open sea.

Moreover, high dissolved Hg concentrations were predicted in some lagoon sites ($\text{Hg} > 10^{-3} \mu\text{g.l}^{-1}$). These potential contaminations should be consolidated by new field measurements. Indeed, these lagoon sites could present significant changes in food concentrations. One of this model's limits is that it does not consider particulate Hg uptake. The inverse analysis should be validated with field studies of metal bioaccumulation kinetics in contaminated sites which are rich in food concentration.

Acknowledgements

This work was supported by the Rhône-Mediterranean-Corsica Water Agency, PACA region and Ifremer. The authors are deeply indebted to Ifremer team of La Seyne sur Mer and Nantes. Drs. Daniel Cossa, Jean-Louis Gonzalez and Mr. Bruno Andral are gratefully acknowledged.

References

- Andral, B., Stanisiere, J.Y., 1999. Réseaux Intégrateurs Biologiques. RINBIO. Evaluation de la qualité des eaux basée sur l'utilisation de stations artificielles de moules en Méditerranée: résultats de la campagne 1998. IFREMER, Toulon, France.
- Andral, B., Stanisiere, J.Y., Sauzade, D., Damier, E., Thebault, H., Galgani, F., Boissery, P., 2004. Monitoring chemical contamination levels in the Mediterranean based on the use of mussel caging. Mar. Pollut. Bull. 49, 704-712.
- Angelidis, M.O., Catsiki, V.A., 2002. Metal bioavailability and bioaccumulation in the marine environment: methodological questions. CIESM Workshop Monograph, Monaco.

- Bacher C., Gangnery, A., 2006. Use of Dynamic Energy Budget and Individual Based models to simulate the dynamics of cultivated oyster populations. J. Sea Res. 51 (this volume).
- Barillé, L., Héral, M., Barillé-Boyer, A.L., 1997. Ecophysiological deterministic model for *Crassostrea gigas* in an estuarine environment. Aquat. Liv. Resour. 10, 31-48.
- Beadman, H.A., Willows, R.I., Kaiser, M.J., 2002. Potential applications of mussel modelling. Helgol. Mar. Res. 56, 76-85.
- Bjerregaard, P., Depledge, M.H., 1994. Cadmium accumulation in *Littorina littorea*, *Mytilus edulis* and *Carcinus maenas*: the influence of salinity and calcium ion concentrations. Mar. Biol. 119, 385-395.
- Boisson, F., Cotret, O., Teyssié, J.L., El-Baradeï, M., Fowler, S.W., 2003. Relative importance of dissolved and food pathways for lead contamination in shrimp. Mar. Pollut. Bull. 46, 1549-1557.
- Boisson, F., Goudard, F., Durand, J.P., Barbot, C., Pieri, J., Amiard, J.C., Fowler, S.W., 2003. Comparative radiotracer study of Cd uptake storage, detoxication and depuration in the oyster *Crassostrea gigas* : potential adaptative mechanisms. Mar. Ecol. Prog. Ser. 254, 177-186.
- Borchardt, T., 1983. Influence of food quantity on the kinetics of cadmium uptake and loss via food and seawater in *Mytilus edulis*. Mar. Biol 76, 67-76.
- Borchardt, T., 1985. Relationship between carbon and cadmium uptake in *Mytilus edulis*. Mar. Biol. 85, 233-244.
- Boyden, C.R., 1977. Effect of size upon metal content of shellfish. J. Mar. Biol. Ass. UK 57, 675-714.
- Casas, S., 2005. Modélisation de la bioaccumulation de métaux traces (Hg, Cd, Pb, Cu et Zn) chez la moule, *Mytilus galloprovincialis*, en milieu méditerranéen. Ph.D. thesis, Université du Sud-Toulon-Var, 314.
- Chiffoleau, J.F., Auger, D., Chartier, E., 2002. Dosage de certains métaux dissous dans l'eau de mer par absorption atomique après extraction liquide-liquide. Editions IFREMER, Plouzané, France.
- Claisse, D., 1989. Chemicals concentration of French coast: the result of ten year mussel watch. Mar. Pollut. Bull. 20, 523-528.
- Claisse, D., Joanny, M., Quintin, J.M., 1992. The French marine pollution monitoring network (RNO). Analusis (Masson, Paris) 20, 19-22.

- Clifton, R.J., Stevens, H.E., Hamilton, E.I., 1983. Concentration and depuration of some radionucleides present in a chronically exposed population of mussels (*Mytilus edulis*). Mar. Ecol. Prog. Ser. 11, 245-256.
- Cossa, D., Bourget, E., Pouliot, D., Piuze, J., Chanut, J.P., 1980. Geographical and seasonal variations in the relationship between trace metal content and body weight in *Mytilus edulis*. Mar. Biol. 58, 7-14.
- Cossa, D., Coquery, M., Naklé, K., Claisse, D., 2002. Dosage du mercure total et du monométhylmercure dans les organismes et sédiments marins. Editions IFREMER, Plouzané, France.
- Dowd, M., 1997. On predicting the growth of cultured bivalves. Ecol. Model. 104, 113-131.
- Evers, E.G., Kooijman, S.A.L.M., 1989. Feeding and oxygen consumption in *Daphnia magna*. A study in energy budgets. Neth. J. Aquat. Biology 39.
- Fisher, H., 1983. Shell weight as an independent variable in relation to cadmium content of molluscs. Mar. Ecol. Prog. Ser. 12, 59-75.
- Fisher, N.S., Teyssié, J.L., Fowler, S.W., Wang, W.-X., 1996. The accumulation and retention of metals in mussels from food and water: a comparison under field and laboratory conditions. Environ. Sci. Technol. 30, 3232-3242.
- Fowler, S.W., 1982. Biological transfer and transport processes. Pollutant transfer and transport in the sea. Kullenberg, G., CRC press. Boca Raton, pp. 2-65.
- Fowler, S.W., Benayoun, G., Small, L.F., 1971. Experimental studies on feeding, growth and assimilation in a Mediterranean euphausiid. Thalassia Jugoslavica 7, 35-47.
- Fowler, S.W., Heyraud, M., La Rosa, J., 1978. Factors affecting methyl and inorganic mercury dynamics in mussels and shrimp. Mar. Biol. 46, 267-276.
- Gangnery, A., Bacher, C., Buestel, D., 2004. Application of a population dynamic model to the Mediterranean mussel, *Mytilus galloprovincialis*, reared in the Thau Lagoon (France). Aquaculture 229, 289-313.
- George, S.G., Coombs, T.L., 1977. The effects of chelating agents on the uptake and accumulation of cadmium by *Mytilus edulis*. Mar. Biol. 39, 261-268.
- Goldberg, E.D., 1975. The Mussel Watch. Mar. Pollut. Bull. 6, 111-113.
- Grant, J., Bacher, C., 1998. Comparative models of mussel bioenergetics and their validation at field culture sites. J. Exp. Mar. Biol. Ecol. 219, 21-44.

- De Kock, W.C., Van het Groenewoud, H., 1985. Modelling bioaccumulation and elimination dynamics of some xenobiotic pollutants (Cd, Hg, PCB, HCB) based on "in situ" observations with *Mytilus edulis*. The Hague.
- Kooijman, S.A.L.M., 1986. Population dynamics on the basis of budgets. The dynamics of physiologically structured populations. Metz, J.A.J., Dickmann, O., Springer Lecture Notes in Biomathematics. Springer Verlag, Berlin, pp. 266-297.
- Kooijman, S.A.L.M., 1988. The von Bertalanffy growth rate as a function of physiological parameters: a comparative analysis. In: Hallam, T.G., Gross, L.J., Levin, S.A. (eds.) Mathematical Ecology. World Scientific, Singapore, pp. 3-45.
- Kooijman, S.A.L.M., 1991. Effects of feeding conditions on toxicity for the purpose of extrapolation. Comp. Biochem. Physiol 100, 305-310.
- Kooijman, S.A.L.M., 1993. Dynamic energy budgets in biological systems, theory and applications in ecotoxicology, Cambridge University Press, Cambridge.
- Kooijman, S.A.L.M., 2000. Dynamic energy and mass budgets in biological systems, Cambridge University Press, Cambridge, 2nd Edition.
- Kooijman, S.A.L.M., Bedaux, J.J.M., 1996. The analysis of aquatic toxicity data. Chemosphere 57, 745-753.
- Kooijman, S.A.L.M., Van Haren, R.J.F., 1990. Animal energy budgets affect the kinetics of xenobiotics. Chemosphere 21, 681-693.
- Langston, W.J., Spence, S.K., 1995. Biological factors involved in metal concentrations observed in aquatic organisms. Environ. Sci. Technol. 26, 407-467.
- Lee, B.G., Luoma, S.N., 1998. Influences of microalgal biomass on absorption efficiency of Cd, Cr and Zn by two bivalves from San Francisco Bay. Limnol. Oceanogr. 43, 1455-1466.
- Lee, B.G., Wallace, W.G., Luoma, S.N., 1998. Uptake and loss kinetics of Cd, Cr and Zn in the bivalves *Potamocorbula amurensis* and *Macoma balthica*: effects of size and salinity. Mar. Ecol. Prog. Ser. 175, 177-189.
- Luoma, S.N., Fisher, N.S., 1997. Uncertainties in assessing contaminant exposure from sediments. In: Ingersoll, C.G., Dillon, T., Biddinger, G.R. (eds.), Ecological risk assessment of contaminated sediments, Pensacola: SETAC Spec. Publ. Series, pp. 211-237.
- Nelder, J.A., Mead, R., 1965. A simplex method for function minimization. Computer Journal 7, 308-313.

- Nisbet, R.M., Muller, E.B., Lika, K., Kooijman, S.A.L.M., 2000. From molecules to ecosystems through dynamic energy budget models. *J. Anim. Ecol.* 69, 913-926.
- Péry, A.R.R., Flammarion, P., Vollat, B., Bedaux, J.J.M., Kooijman, S.A.L.M., Garric, J., 2002. Using a biology based model (Debtox) to analyse bioassays in ecotoxicology: opportunities and recommendations. *Environ. Toxicol. Chem.* 21, 459-465.
- Popham, J.D., D'auria, J.M., 1983. Combined effect of body size, season and location on trace element levels in mussels (*Mytilus edulis*). *Arch. Envir. Contam. Toxic.* 12, 1-14.
- Pouvreau, S., Bacher, C., Héral, M., 2000. Ecophysiological model of growth and reproduction of the black pearl oyster, *Pinctada margaritifera*, in the planktonic food web of Takapoto lagoon (French Polynesia). *Aquaculture* 186, 117-144.
- Pouvreau, S., Bourles, Y., Lefebvre, S., Gangnery, A., Alunno-Bruscia, M. Application of a dynamic energy budget model to the Pacific oyster, *Crassostrea gigas*, reared under various environmental conditions. *J. Sea Res.* 51 (this volume).
- Rainbow, P.S., Phillips, D.J.H., Depledge, M., 1990. The significance of trace metal concentrations in marine invertebrates. A need for laboratory investigation of accumulation strategies. *Mar. Pollut. Bull.* 21, 321-324.
- Ren, J.S., Ross, A.H., 2001. A dynamic energy budget model of the Pacific oyster *Crassostrea gigas*. *Ecol. Model.* 142, 105-120.
- Riget, F., Johansen, P., Asmund, G., 1997. Uptake and release of lead and zinc by blue mussels (*Mytilus edulis*). Experience from transplantation experiments in greeland. *Mar. Pollut. Bull.* 34, 805-815.
- Roditi, H.A., Fisher, N.S., 1999. Rates and routes of trace element uptake in zebra mussels. *Limnol. Oceanogr.* 44, 1730-1749.
- Roditi, H.A., Fisher, N.S., Sanudo-Wilhelmy, S.A., 2000. Field testing a metal bioaccumulation model for zebra mussels. *Environ. Sci. Technol.* 34, 2817-2825.
- Roditi, H.A., Fisher, N.S., Sanudo-Wilhelmy, S.A., 2000. Uptake of dissolved organic carbon and trace elements by zebra mussels. *Nature* 407, 78-80.
- Roesijadi, G., Young, J.S., Drum, A.S., Gurtisen, J.M., 1984. Behaviour of trace metals in *Mytilus edulis* during a reciprocal transplant field experiment. *Mar. Ecol. Prog. Ser.* 18, 155-170.
- Rouillon, G., Navarro, E., 2003. Differential utilisation of species of phytoplankton by the mussel *Mytilus edulis*. *Acta Oecologica* 24, 299-305.

- Schulz-Baldes, M., 1977. Lead transport in the common mussel *Mytilus edulis*. Proc. Int. Conf., natl. res. Council Can., Vol 2 pp. 211.
- Sunda, W.G., Huntsman, S.A., 1998. Processes regulating cellular metal accumulation and physiological effects: Phytoplankton as model systems. The Science of the Total Environment 219, 165-181.
- Thomann, R.V., Mahony, J.D., Mueller, R., 1995. A steady-state model of biota sediment accumulation factor for metals in two marine bivalves. Environ. Toxicol. Chem. 14, 1989-1998.
- Van der Veer H. W., Cardoso, J.F.M.F., Van der Meer, J. Estimation of DEB parameters for various North Atlantic bivalve species. J. Sea Res. 51 (this volume).
- Van Haren, R.J.F., Schepers, H.E., Kooijman, S.A.L.M., 1994. Dynamic energy budgets affect kinetics of xenobiotics in the marine mussel *Mytilus edulis*. Chemosphère 29, 163-189.
- Wang, W.-X., Dei, R.C.H., 1999. Factors affecting trace element uptake in the black mussel *Septifer virgatus*. Mar. Ecol. Prog. Ser. 186, 161-172.
- Wang, W.-X., Fisher, N.S., 1997. Modeling the influence of body size on trace element accumulation in the mussel *Mytilus edulis*. Mar. Ecol. Prog. Ser. 161, 103-115.
- Wright, D.A., 1995. Trace metal and major ion interactions in aquatic animals. Mar. Pollut. Bull. 31, 8-18.

Table 1. Main variables of the Dynamic Energy Budget model. Notation after Kooijman (2000).

	Unit	Description
V	cm ³	Structural volume
E	J	Energy reserves
R	J	Energy allocated to development and reproduction
W	g	Fresh tissue mass
X	µg l ⁻¹	Food concentration
C_d	µg l ⁻¹	Water metal concentration
C_p	mg kg ⁻¹	Food metal concentration
C_w	mg kg ⁻¹	Mussel metal concentration

Table 2. Parameters of the Dynamic Energy Budget model. Notation after Kooijman (2000).

	Unit	Description	Value	Reference
T_A	K	Arrhenius temperature	5800	Van der Veer et al. (2006)
T_1	K	Reference temperature	293	Van der Veer et al. (2006)
T_L	K	Lower boundary of tolerance range	275	Van der Veer et al. (2006)
T_H	K	Upper boundary of tolerance range volume	296	Van der Veer et al. (2006)
T_{AL}	K	Rate of decrease of lower boundary	45430	Van der Veer et al. (2006)
T_{AH}	K	Rate of decrease of upper boundary	31376	Van der Veer et al. (2006)
ρ	-	Losses due to digestion	0.2	Kooijman, 2000
$\{\dot{p}_{Am}\}$	J.cm ⁻² .d ⁻¹	Maximum surface area-specific assimilation rate	147.6	Van der Veer et al. (2006)
$[\dot{p}_M]$	J.cm ⁻³ .d ⁻¹	Volume specific maintenance costs	24	Van der Veer et al. (2006)
$[E_m]$	J.cm ⁻³	Maximum energy density	2190	Van der Veer et al. (2006)
$[E_G]$	J.cm ⁻³	Volume-specific costs of growth	1900	Van der Veer et al. (2006)
μ_E	J.g ⁻¹	Energy content of reserves	6750	Casas (2005)
κ	-	Fraction of utilised energy spent on maintenance/growth	0.7	Van der Veer et al. (2006)
m	-	Shape coefficient	calibration	
V_p	cm ³	Volume at start of reproductive stage	0.06	Van der Veer et al. (2006)
X_K	µg.L ⁻¹	Half saturation coefficient	calibration	

d	g.cm^{-3}	Specific density	1	
\dot{r}_{da}	$\text{L.cm}^{-2}.\text{day}^{-1}$	Uptake rate from water	calibration	
\dot{r}_{pa}	$\text{g.cm}^{-2}.\text{day}^{-1}$	Uptake rate from food	calibration	
\dot{r}_{ad}	$\text{g.cm}^{-2}.\text{day}^{-1}$	Elimination rate	calibration	

Table 3. Comparison of dissolved trace metal concentration measured during experiment and predicted by inverse method applied to the RINBIO network.

Location	Dissolved Hg, Water ($10^{-3} \mu\text{g.l}^{-1}$)		Dissolved Pb, Water ($10^{-3} \mu\text{g.l}^{-1}$)	
	measured Min-Max	predicted	measured Min-Max (mean)	Predicted
Lazaret bay	1-3	2.1	19-190 (111)	107
Bages Lagoon	0.3-0.8	0.47	8-50	17
Port-Cros island	0.2-0.5	0.25	0.1-26	13

Figure 1. Map of artificial mussel sites in the open sea (sites 2-49) and in lagoons (sites 80-90) of the French Mediterranean Sea (ns: site number in RINBIO network). Description of 3 sites: Bages lagoon ($43^{\circ}04.70' N$, $3^{\circ}00.00' E$, site 80), Lazaret bay ($43^{\circ}05.40' N$, $5^{\circ}54.50' E$, site 31) and Port-Cros island ($43^{\circ}00.91' N$, $6^{\circ}23.41' E$, site 35) (C.Tomasino).

Figure 2. Schematic representation of the experimental design, made of 4 datasets corresponding to different mussel population surveys. Populations were setup at 2 different contaminated sites (Lazaret et Bages), and transferred to a decontamination site (Port-Cros). For each contaminated sites, long (6 months) and short (3 months) time exposure were tested.

Figure 3. Schematic representation of the energy flow through an organism in the DEB model (Kooijman, 2000), and contaminants bioaccumulation. 1: assimilation, 2: utilisation

Figure 4. Hydrological data during the mussel growth experiments.

- a: temperature ($^{\circ}C$) in three sites
- b: chlorophyll-a and pheopigment concentrations ($\mu g.l^{-1}$) in Lazaret bay;
- c: in Bages lagoon and
- d: in Port-Cros island.

Figure 5. Observed (closed symbols: long exposure; open symbols: short exposure) mussel growth (fresh tissue mass, g) during contamination in Lazaret bay and Bages lagoon (mid September to mid March) and during decontamination in Port-Cros island (mid March to mid June), together with growth simulated with the DEB model (lines).

Figure 6. Observed concentration of Hg (upper graph) and Pb (lower graph) ($mg kg^{-1}$ dry weight) in *Mytilus galloprovincialis* during short (open symbols) and long (closed symbols) contamination in Lazaret bay (square symbols) and Bages lagoon (triangle symbols) and subsequent decontamination in Port-Cros island together with DEB model simulation (line).

Figure 7. *Mytilus galloprovincialis* at artificial mussel sites in the open sea (sites 2-49) and in lagoons (sites 80-90) of the French Mediterranean Sea (ns: site number in RINBIO network). For locations see also Fig. 1.

- a: Measured dry tissue mass (g)
- b: Estimated functional response (f , -).
- c: dissolved concentration of Hg in water (10^{-3} $\mu\text{g.L}^{-1}$),
- d: dissolved concentration of Pb in water (10^{-3} $\mu\text{g.l}^{-1}$),

Estimations are the results of inverse analysis by means of the DEB model.
for more information see text

Figure 1

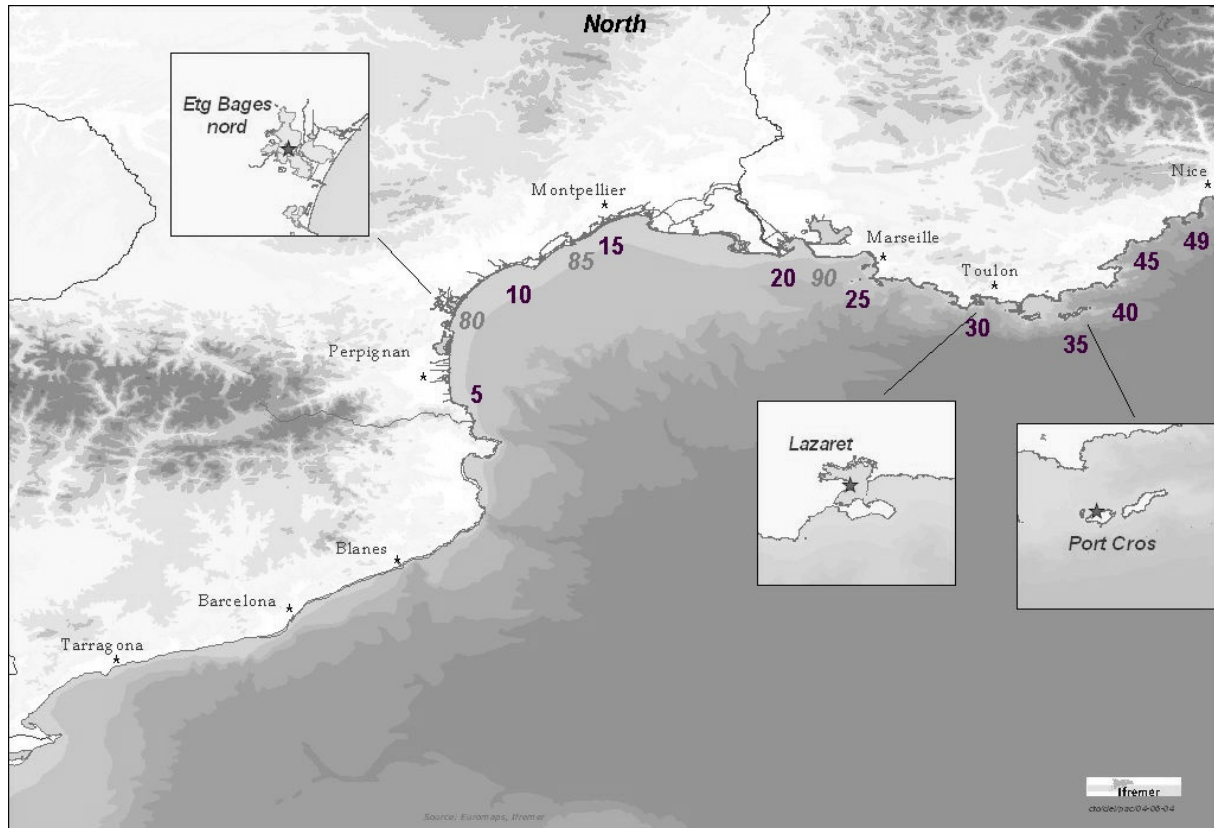


Figure 2

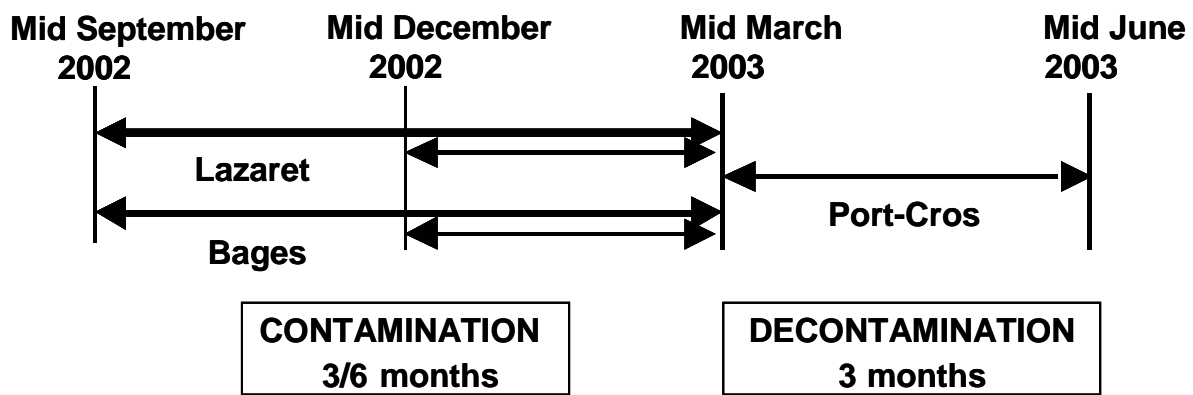


Figure 3

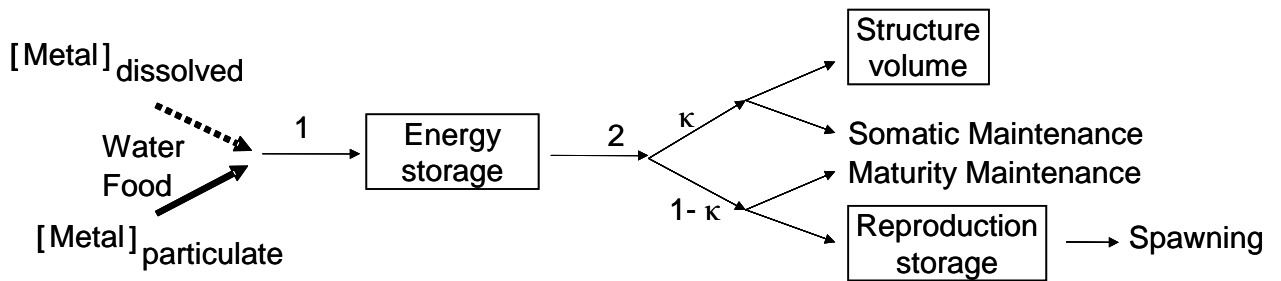
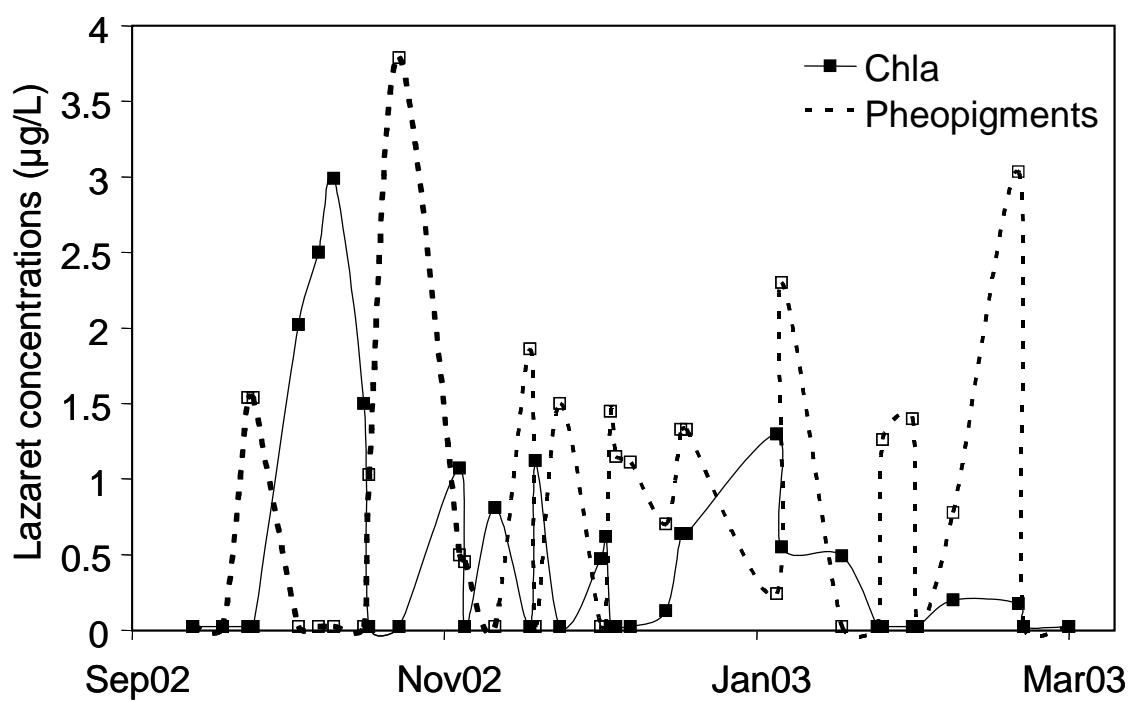
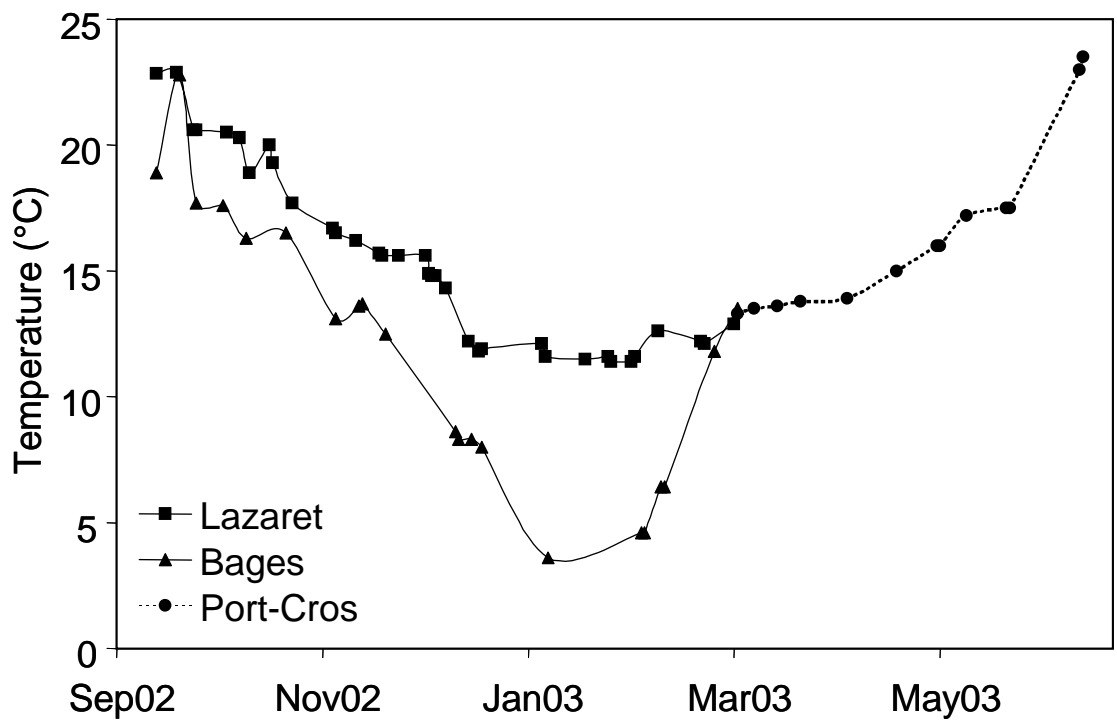


Figure 4



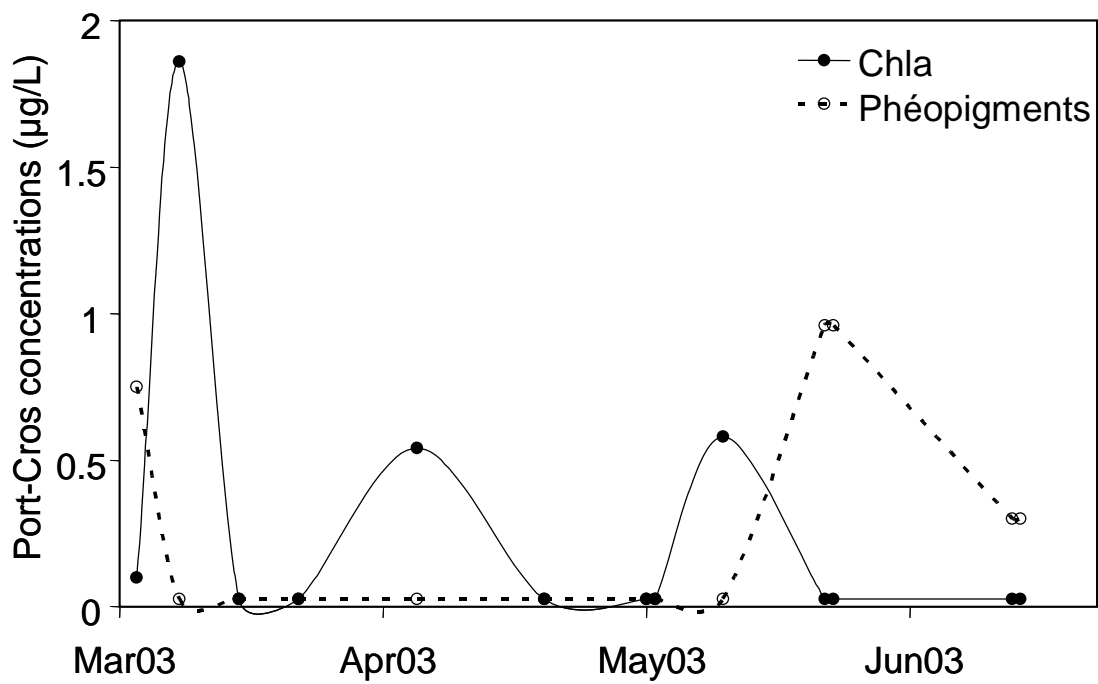
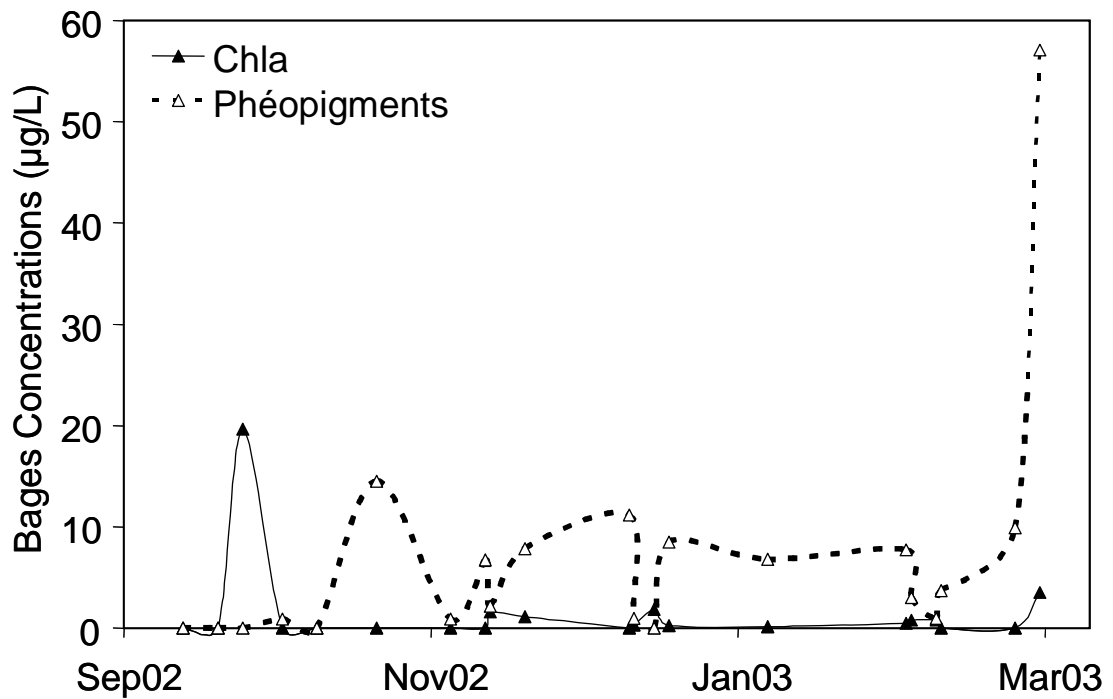


Figure 5

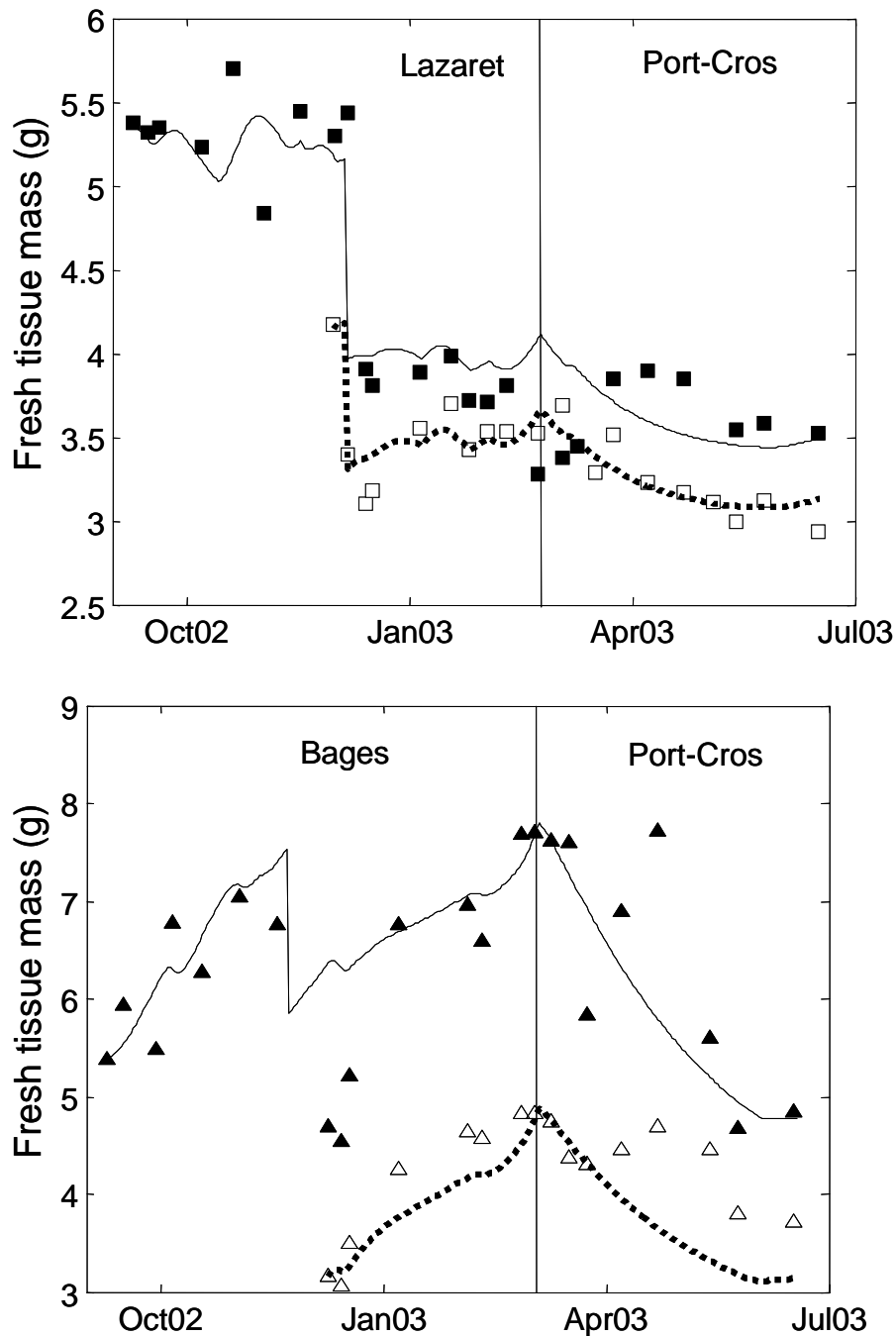


Figure 6

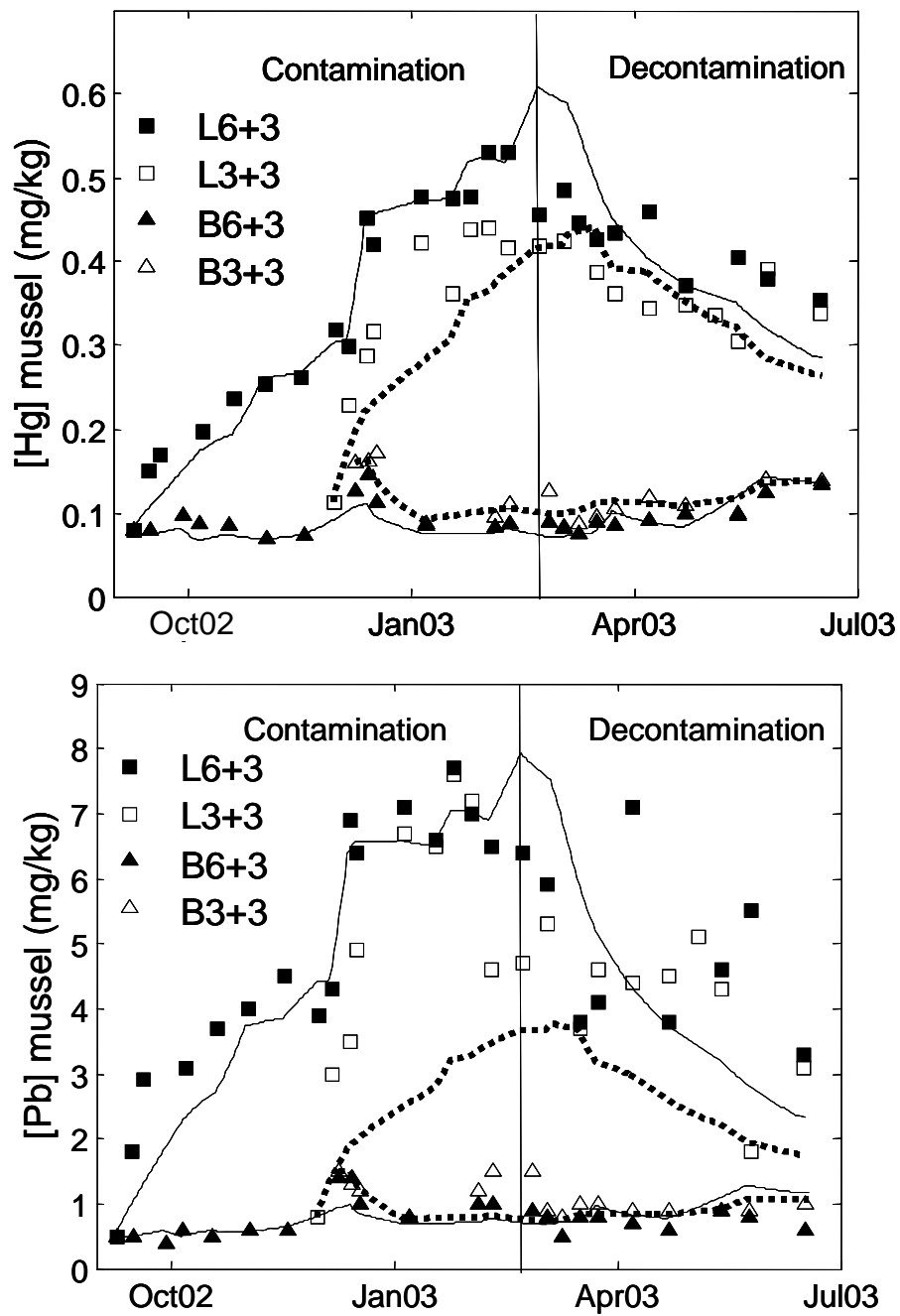


Figure 7

